Photoneutron cross sections for ^{14}C

R. E. Pywell
Saskatchewan Accelerator Laboratory, University of Saskatchewan, Saskatoon, Saskatchewan, Canada S7N 0W0

B. L. Berman
Lawrence Livermore National Laboratory, University of California, Livermore, California 94550
and Department of Physics, George Washington University, Washington, D.C. 20052

J. G. Woodworth
Lawrence Livermore National Laboratory, University of California, Livermore, California 94550

J. W. Jury
Department of Physics, Trent University, Peterborough, Ontario, Canada K9J 7B8

K. G. McNeill
Department of Physics, University of Toronto, Toronto, Ontario, Canada M5S 1A7

M. N. Thompson
School of Physics, University of Melbourne, Parkville, Victoria, Australia 3052
(Received 29 March 1985)

The photoneutron cross sections for ^{14}C [$\sigma(\gamma,1n)$ and $\sigma(\gamma,2n)$] have been measured up to 36 MeV using monochromatic photons. The cross section for the emission of a single neutron displays a very prominent resonance near 15 MeV which appears to decay primarily to the ground state of ^{13}C. The $(\gamma,2n)$ cross section is sharply peaked at 26 MeV and is large compared with those for ^{12}C and ^{13}C. The integrated total photoneutron cross section up to 36 MeV is 126 ± 12 MeV mb (61% of the Thomas-Reiche-Kuhn sum-rule value). The ^{14}C photoneutron cross sections are interpreted in terms of the reaction kinematics and the competition among the particle channels in order to provide information on the isospin properties of the major $E1$ states in ^{14}C and on the validity of the weak core-coupling model.

I. INTRODUCTION

The present experiment is part of a systematic study of photonuclear reactions in light nuclei at or near closed shells or subshells. These experimental investigations have included photoneutron studies in the following three series: (a) ^{12}C and ^{13}C;[1,2] (b) ^{15}N, ^{16}O, ^{17}O, and ^{18}O;[3–8] and (c) ^{28}Si, ^{29}Si, and ^{30}Si.[9–11] This experiment extends the first series to include ^{14}C. Photoproton studies have been carried out on many of these nuclei, including ^{13}C, ^{16}O, ^{18}O, and, recently, ^{17}O.[12,13,7,8,14]

The general picture that has emerged from these measurements is that the photonuclear cross section for a nucleus with one or two nucleons outside a shell exhibits a giant dipole resonance (GDR) which is a modified version of that of the core nucleus. In addition, there is a pygmy resonance which is attributable to the excitations of the "valence" neutrons which are weakly coupled to the core.

In the conventional view, ^{14}C is regarded as consisting either of a ^{12}C core with two $p_{1/2}$ valence neutrons or of an ^{16}O core with two $p_{1/2}$ proton holes. In this view ^{15}N, whose photoneutron cross section has already been measured in this series,[3] can be regarded as ^{16}O with one proton hole. On the other hand, ^{14}C may be regarded as a nucleus that has a closed $p_{3/2}$ (sub)shell of protons as well as its closed $p_{1/2}$ shell of neutrons. In order to understand the structure of ^{14}C it is essential to know to what extent either of these pictures is a valid description. One reason for this study of the photoexcitation of ^{14}C is to attempt to address this question.

Experimentally, ^{14}C has been studied by electron scattering,[15] by radiative neutron capture on ^{13}C,[16] and by neutron elastic scattering.[17] The electron-scattering work looked primarily at $M1$ transitions (180° scattering of electrons). Of particular interest to the present study is a peak at 11.31 MeV, assigned a spin and parity of 1^+ and a measured electromagnetic transition width of 6.8 ± 1.4 eV. Subsequent to the measurement reported here there has been a measurement of the (γ,n_0) channel,[18] which also shows a peak at 11.3 MeV, as well as (at some angles) satellite resonances on either side of it. The (γ,n_0) cross section also indicates considerable transition strength at an excitation energy of about 15 MeV.

The Thomas-Reiche-Kuhn (TRK) sum-rule value for the total integrated photoabsorption cross section is $60NZ/A=206$ MeV mb. Experience with other nuclei in this region indicates that, up to an energy of 30 MeV, about 60% to 70% of this sum-rule value is exhausted.

Photoreactions in the $A=14$ nuclei have been investigated theoretically by Kissener *et al.*,[19] by Vergados,[20] and recently by Assafiri and Morrison.[21] Because ^{14}C has a ground-state isospin $T_0=1$, it is expected that both

$T_< = T_0 = 1$ and $T_> = T_0 + 1 = 2$ states will be excited by photon absorption. The splitting of the GDR into its $T_<$ and $T_>$ components and the relative strengths of these two components has been discussed generally in the papers referenced above. For the case of ^{14}C, Goulard and Fallieros[22] predict that the centroids of the two isospin components of the GDR are separated by 8.6 MeV and that their relative strengths are approximately equal.

The energetics of the photoreactions for ^{14}C are shown schematically in Fig. 1 and the reaction thresholds are listed in Table I. The (γ,n) threshold energy is relatively low, as is the $(\gamma,2n)$ threshold. On the other hand, the (γ,p) threshold is very high, and therefore, in the excitation-energy region where the main $T_<$ component of the GDR is expected to lie, photoproton emission is energetically impossible. Photoneutron emission from the $T_>$ component of the GDR to the 15.11-MeV ($T=\frac{3}{2}$) state of ^{13}C is allowed. This state can, because of its isospin impurity, decay by neutron emission to low-lying states of ^{12}C and thus contribute to the $(\gamma,2n)$ reaction channel. The (γ,pn) threshold is at 25.7 MeV, and this channel [which is included in the $(\gamma,1n)$ channel of the present measurement] can compete with the (γ,p) reaction, particularly because there exist only a few levels of ^{13}B below an excitation energy of 5 MeV.

In view of the above considerations, two-neutron emission from the $T_<$ part of the GDR might be expected to be relatively small, since (γ,n) transitions to low-lying states should predominate because of energy considerations. In addition, the (γ,p) reaction is expected to compete above about 21 MeV. However, once $T=\frac{3}{2}$ states become available in the first daughter nucleus (^{13}C), the $(\gamma,2n)$ process should become more probable. The opening of the (γ,pn) channel at 25.7 MeV is expected to reduce the proportion of reactions via the $(\gamma,2n)$ channel and thus initiate a reduction in the latter cross section.

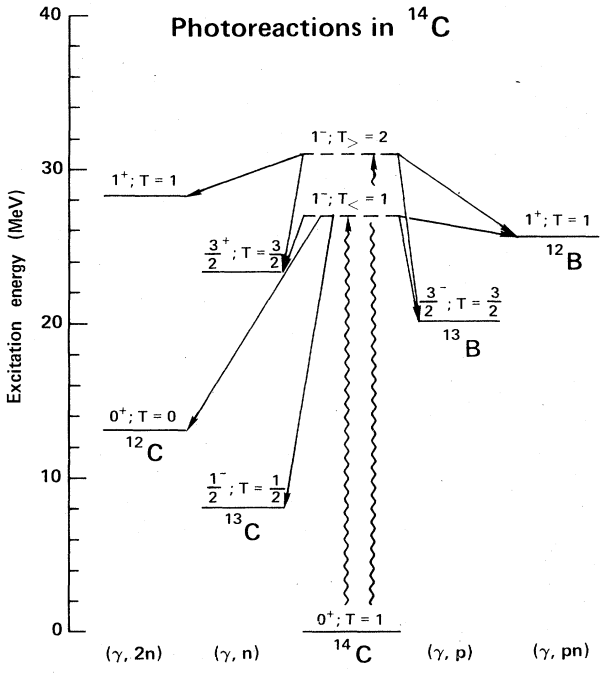

FIG. 1. A schematic energy-level diagram, showing the various transitions and residual nuclei involved, for the photoreactions in ^{14}C.

TABLE I. Reaction thresholds for ^{14}C.[a]

Reaction	Threshold (MeV)
^{14}C(γ,n)	8.18
^{14}C(γ,α)	12.01
^{14}C$(\gamma,2n)$	13.12
^{14}C$(\gamma,\alpha n)$	18.83
^{14}C(γ,p)	20.83
^{14}C(γ,d)	23.49
^{14}C(γ,pn)	25.71
^{14}C$(\gamma,p2n)$	29.08
^{14}C$(\gamma,3n)$	31.84
^{14}C$(\gamma,2p)$	36.59

[a]From Ref. 23.

The question of the core-coupling effects in ^{14}C is of quite general interest. The two extreme cases are (a) a weak-coupling model which might lead to a structured pygmy resonance at low energies and a ^{12}C-like GDR near 23 MeV, and (b) a strongly collective model which might predict a "closed-shell" ^{14}C GDR split by isospin into roughly equal components. For the weak-coupling case, although a prominent and structured pygmy resonance would be expected, it would be smaller than that observed for ^{18}O,[7,8] where more single-particle transitions are available involving valence neutrons in the *s-d* shell. Therefore, the present measurement of the photoneutron cross sections for ^{14}C, in conjunction with the previous results for the other nuclei in this study, attempts to determine the extent to which the weak-coupling model is applicable. Preliminary results of this work appeared in Ref. 27.

II. EXPERIMENTAL PROCEDURE

A detailed description of the experimental procedure has been given previously,[7] and therefore only its major features will be summarized here.

A 120-MeV electron beam from the Lawrence Livermore National Laboratory electron-positron linear accelerator was incident on a tungsten-rhenium positron converter. The positrons were analyzed in momentum to $\sim 1\%$ and were then incident on a 0.76-mm-thick beryllium annihilation target, where both annihilation photons and bremsstrahlung radiation were produced. The transmitted positrons were swept away with a dump magnet. The photons then passed through a calibrated transmission ion chamber (which served as a photon flux monitor) before being incident on the sample, which was placed at the center of a 4π neutron detector. The neutron detector consisted of a 0.61-m cube of paraffin containing 48 high-pressure BF_3 tubes arranged in four concentric rings. Because of the neutron moderation in the paraffin, the ratio of the number of neutron counts

recorded in the outer ring to that in the inner ring (the ring ratio) gives a measure of the average neutron energy (and therefore of the detector efficiency) for each data point.

Two ^{14}C samples were used in this experiment. One consisted of 9.22 g of elemental carbon enriched in ^{14}C to 84% by mass (7.77 g of contained ^{14}C). The other consisted of an 84.1-g sample in the form of calcium carbonate ($CaCO_3$), the carbon content of which was enriched in ^{14}C to 83% by mass (9.45 g of contained ^{14}C). These samples were packed in aluminum cylinders 3.8 cm in diameter. A similar container, in which 1.45 g of ^{12}C was placed, was used as a sample blank in order to determine the neutron background from the container and the contribution from the ^{12}C impurity in the samples. The samples were placed in a pneumatic sample changer so that they could be inserted and removed remotely. Special precautions and monitoring procedures had to be followed because of the radioactive nature of ^{14}C, whose activity is approximately 63 Ci/mole.

The experimental procedure for each photon energy consisted of measuring the photoneutrons from the ^{14}C sample and from the sample blank, both with and without the annihilation target present. In order to determine and subsequently subtract out the yield of photoneutrons produced by the positron bremsstrahlung, the measurements were repeated using an electron beam instead of a positron beam. A multiplicity analysis of these data enabled the $(\gamma,1n)$ and $(\gamma,2n)$ cross sections to be extracted simultaneously and independently.

Three separate sets of data were obtained during two experimental running periods:

1. In the first running period the elemental-carbon sample was used for measurements in the photon-energy range from 15 to 19 MeV in approximately 200-keV steps, and from 23 to 36 MeV in 400-keV steps.

2. In the second running period the elemental-carbon sample was used for measurements in the photon-energy range from 19 to 27 MeV in 200-keV steps.

3. Also in the second running period, a sample combining the elemental-carbon and calcium-carbonate samples was used for measurements in the photon-energy range from 8 to 16 MeV in 100-keV steps. This energy range is below the energy for which there is a significant contribution due to photoneutrons from the oxygen and calcium present in this combined sample.

These three sets of data were analyzed independently using the steps summarized below (for details see Refs. 7). First, the number of neutron events for each yield measurement was corrected for pileup of counts in the detector. Then the neutron and ion-chamber backgrounds, as measured with the annihilation-target-out runs, were subtracted from both the positron and electron yield measurements. These backgrounds were dependent upon whether or not the ^{14}C sample was in place, owing to the radioactivity of the sample. The electron data were fitted with a smooth curve; then the value of this fitted curve at the energy of each positron yield point, multiplied by the appropriate normalization factor, was subtracted from the positron yield in order to obtain the yield from the annihilation photons alone. The appropriately normalized yield from the sample blank (which included ^{12}C) then was subtracted to give the net yield from ^{14}C for each of the three data sets.

From these yield data the absolute photoneutron cross sections for each data set were obtained. The procedure for doing this involved (a) a correction for the neutron multiplicity in order to ascertain the true number of single- and double-photoneutron events, (b) a correction for the detector efficiency at each energy, derived from the measured ring ratio, (c) a correction for the (atomic) attenuation of photons in the sample, and finally (d) the conversion into cross-section units using the calibrated ion-chamber response per annihilation photon and the number of ^{14}C nuclei irradiated by the photon beam.

Figures 2(a) and (b) show the results of this analysis for the three separate data sets. It can be seen that sets 1 and 2 (both of which used the same sample) agree well, while there is a 5% to 10% disagreement between set 3 and the other two. This disagreement is of the same order as the uncertainty in the mass of ^{14}C in either of the samples ($\sim$5%). We therefore decided to normalize sets 1 and 2 up, and set 3 down, to the average value of the cross section in the overlap region. The combined data set was then binned at intervals consistent with the energy resolution of the annihilation photons at each beam energy,

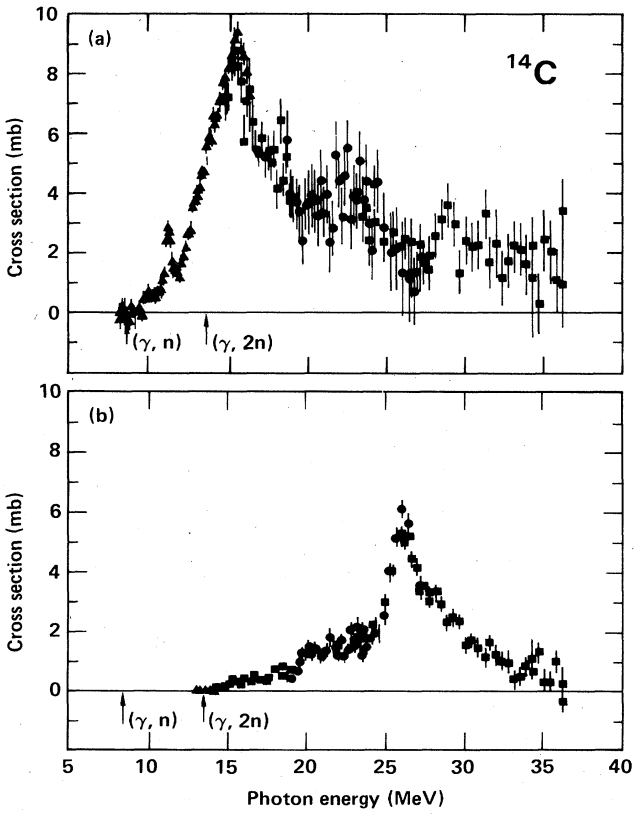

FIG. 2. Data sets 1, 2, and 3 for (a) the $(\gamma,1n)$ and (b) the $(\gamma,2n)$ cross sections for ^{14}C (squares, set 1; circles, set 2; triangles, set 3). The arrows represent the threshold energies for the $(\gamma,1n)$ and $(\gamma,2n)$ reactions.

which ranges from 200 keV at the lowest energy measured to 400 keV at the highest energy. Figure 3 shows the results of this analysis. The error bars shown in the figures are statistical only; the uncertainty in the absolute cross section does not exceed 10%; it results mainly from the normalization uncertainty discussed above and from the ~5% uncertainty in the absolute photon flux.

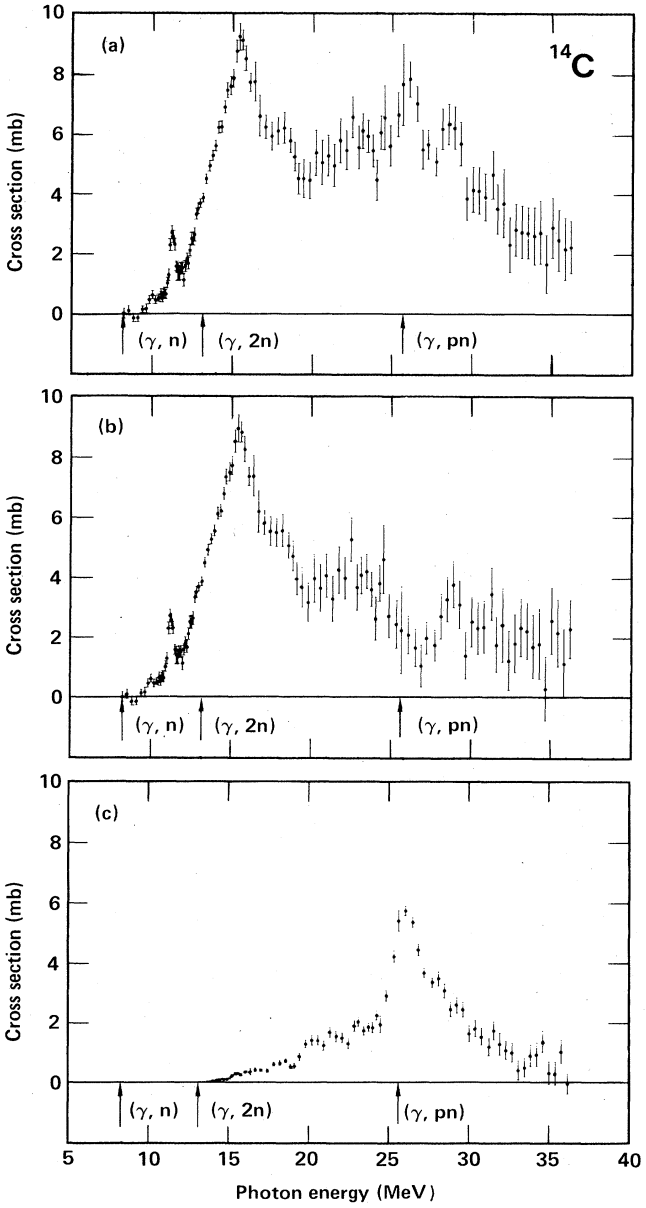

FIG. 3. Present results for the photoneutron cross sections for ^{14}C: (a) the total photoneutron cross section $\sigma(\gamma,n_{tot})=\sigma[(\gamma,n)+(\gamma,pn)+(\gamma,\alpha n)+(\gamma,2n)]$; (b) $\sigma(\gamma,1n)=\sigma[(\gamma,n)+(\gamma,pn)+(\gamma,\alpha n)]$; (c) $\sigma(\gamma,2n)$. The plotted error bars indicate the statistical uncertainties only. The uncertainty in the absolute cross section does not exceed 10%. The arrows represent the threshold energies for the (γ,n), $(\gamma,2n)$, and (γ,pn) reactions.

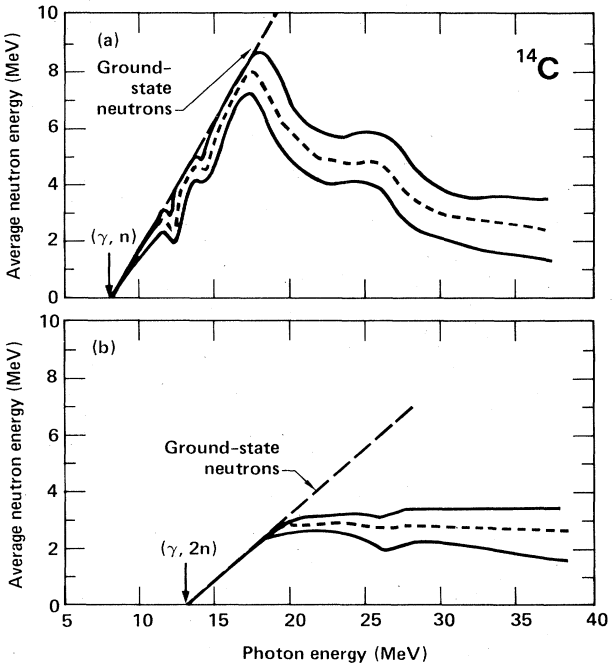

FIG. 4. The average energy of the emitted photoneutrons, as determined by the ring-ratio technique, plotted against photon energy, for (a) the $(\gamma,1n)$ reaction and (b) the $(\gamma,2n)$ reaction. The short-dashed lines show the best fit to the data; the band between the solid lines represents the approximate statistical uncertainty in the data points; the long-dashed lines show the neutron energy that would be obtained for purely ground-state transitions.

To ensure that our estimate of the absolute uncertainty was realistic, we carried out a measurement of the cross section of the reaction $^{141}Pr(\gamma,n_{tot})$ during the course of the ^{14}C measurement reported here. Using a sample of ^{141}Pr metal, measurements were made at 11 different photon energies ranging from 12 to 17 MeV, spanning the peak of the GDR. Data were recorded and processed in an identical fashion as for the ^{14}C samples. At all energies, the measured cross-section values were seen to agree with previous measurements from a number of experiments[24] to within 3%.

The average energy of the emitted photoneutrons can be ascertained from the ring ratio (e.g., see Refs. 7). The best fits to these data are shown in Figs. 4(a) and (b) for the $(\gamma,1n)$ and $(\gamma,2n)$ reactions, respectively.

III. RESULTS AND DISCUSSION

The results of this experiment are shown in Figs. 3–6. Figure 3(a) shows the total photoneutron cross section $\sigma(\gamma,n_{tot})=\sigma[(\gamma,1n)+(\gamma,2n)]$ plotted as a function of the energy of the incident photon beam. Figure 3(b) shows the single photoneutron cross section $\sigma(\gamma,1n)=\sigma[(\gamma,n)+(\gamma,pn)+(\gamma,\alpha n)]$ on the same scale, and Fig. 3(c) shows the $(\gamma,2n)$ cross section.

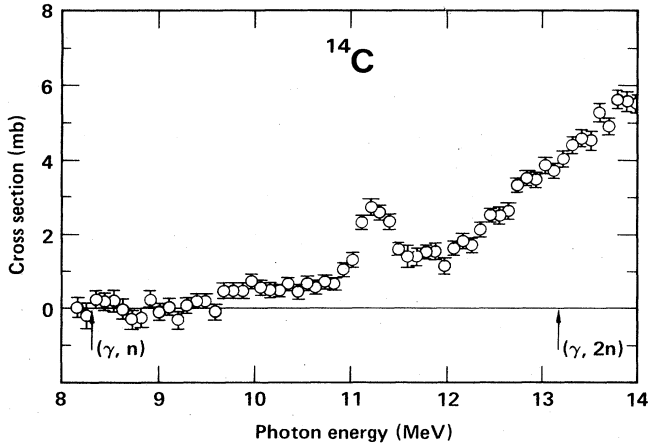

FIG. 5. An expanded-scale plot of the single-photoneutron cross section of Fig. 3(b) below 14 MeV, showing the structure in the low-energy region.

A. The single photoneutron cross section

Figure 3(b) shows the cross section for reactions in which a single neutron is emitted following photon absorption by ^{14}C. Figure 4(a) shows the measured average energy of the emitted photoneutrons as a function of the incident photon energy. The features of this cross section are discussed for four photon-energy regions in the following subsections.

1. Excitation energies below 14 MeV

The $(\gamma,1n)$ cross section in the energy region below 14 MeV is shown in Fig. 5. There is evidence for a small peak near 10 MeV, which kinematically must result from photoneutron transitions to the ground state of ^{13}C. The average-neutron-energy data confirm this [Fig. 4(a)]. Weak states at 9.8 and 10.5 MeV have been observed by 180° inelastic electron scattering,[15] and a distinct 0^+ state at $E_x=9.746$ MeV has been seen in the ^{12}C(t,p)^{14}C measurement of Mordechai *et al.*[25] The fact that very little strength is seen in the present experiment at these energies is not surprising because such 0^+ states are expected[17] to be made up of two neutrons in the *s-d* shell coupled to a ^{12}C core. Such states would manifest themselves much more readily in the ^{12}C(t,p)^{14}C reaction than in the ^{14}C(γ,n) reaction, which favors $E1$ transitions at low momentum transfers.

The prominent state seen at 11.25 ± 0.05 MeV must, from kinematic considerations, also decay to the ground state of ^{13}C (transitions to the first excited state at 3.09 MeV in ^{13}C are not allowed until an excitation energy in ^{14}C of 11.27 MeV). A recent measurement of the ground-state reaction ^{14}C(γ,n_0) (Ref. 18) using the photoneutron-time-of-flight technique also reveals a peak at 11.3 MeV. When the area of this peak is converted to the total-cross-section scale, good agreement is found with the area of the peak seen in the present experiment. The 180°-electron-scattering data of Crannell *et al.*[15] exhibit a 1^+ state at 11.31 MeV, of total width 207 ± 13 keV, excited by a strong $M1$ transition from the 0^+ ground state of ^{14}C. The angular distribution of the 11.3-MeV state observed in the ground-state photoneutron measurement displays a pronounced $E1$-$M1$ interference, suggesting that it may be identified with the 11.31-MeV peak reported by Crannell *et al.* and with the 11.25-MeV peak seen in this experiment. A 1^+ state at $E_\gamma=11.29$ MeV, with a total neutron width of about 180 keV, has also been seen in the high-resolution elastic-neutron-scattering data of Lane *et al.*[17] However, the large angular asymmetries imply that this state is not pure $M1$. This is consistent with the present measurement, which displays (in this en-

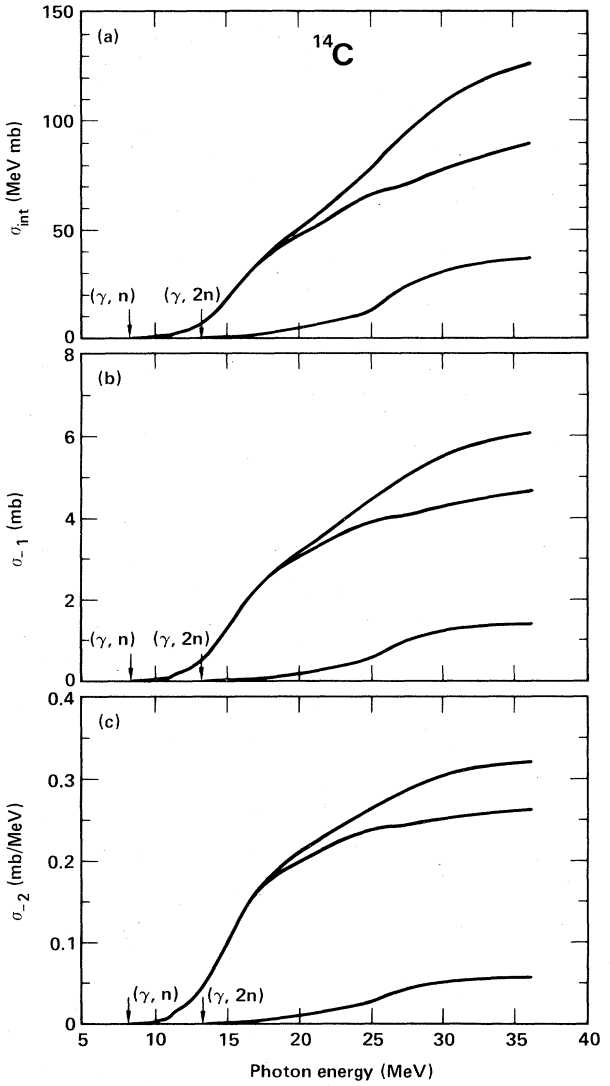

FIG. 6. The integrated photoneutron cross sections for ^{14}C, and their moments, are plotted as functions of the upper limit of integration. Part (a) shows the integrated cross sections σ_{int} for $\sigma(\gamma,2n)$ (bottom curve), $\sigma(\gamma,1n)$ (middle curve), and their sum, $\sigma(\gamma,n_{tot})$ (top curve). Integrated cross sections over any desired limits can be obtained from these curves by subtraction. Parts (b) and (c) show the energy-weighted moments of the integrated cross sections σ_{-1} and σ_{-2} (as defined in the text), respectively.

ergy region) an underlying continuum cross section of about 1 mb in the low-energy tail of the GDR.

The electron-scattering results of Crannell *et al.*[15] show the electromagnetic transition width, Γ_{γ_0}, for this 11.3-MeV state to be 6.8 ± 1.4 eV. The results of the present experiment (after the GDR tail is subtracted) show an integrated value of the cross section for this state of 1.1 ± 0.1 MeV mb, which yields a value for Γ_{γ_0} of 12 ± 1 eV. The disagreement of these two results, together with the $E1$-$M1$ interference seen in the ground-state-photoneutron measurement, implies that the observed peak at 11.25 MeV is a mixture of $M1$ and $E1$ strength. However, it appears that a great deal of the total $M1$ strength for ^{14}C is concentrated at this energy. As noted by Crannell *et al.*, this has important consequences for the understanding of the coupling of valence nucleons. In other cases, such as ^{11}B, ^{22}Ne, and ^{24}Mg, the extra-core neutrons are responsible for the fragmentation of the $M1$ strength into many states. For the case of ^{14}C, the $M1$ strength of the ^{12}C "core" appears not to be fragmented, but remains intact in the 11.3-MeV peak.

Immediately above this state, in the energy region from 11.3 to 12.8 MeV, there is a significant dip in the average neutron energy [see Fig. 4(a)]. This dip indicates the presence of states in ^{14}C (not readily seen in the cross section because of the dominance of the GDR tail) that decay to one or more of the two bound excited states ($J^\pi=\frac{1}{2}^+$ and $\frac{3}{2}^-$) at 3.09 and 3.68 MeV in ^{13}C. The energy of the emitted neutrons is seen to be reduced from 3.5 MeV (which it would be for 100% ground-state transitions) to about 2.5 MeV. Such an average energy would be obtained if there were states in this energy region which had a combined cross section of about 0.5 mb, and which decayed to one or both of these two states in ^{13}C by emitting neutrons with an average energy of about 1 MeV. The $\frac{3}{2}^-$ state at 3.68 MeV is a reasonable candidate for most of the transition strength because it is the only negative-parity state in this region; the dominant $E1$ transitions involving the single-particle excitation of a $p_{3/2}$ neutron would proceed naturally through this state.

Another deviation from purely ground-state transitions is observed near an excitation energy of 14 MeV, where the average neutron energy again dips by about 1 MeV.

Discounting the state at 11.3 MeV because of its special ($M1$-$E1$) nature, there is little evidence for a distinct and highly structured pygmy resonance as seen, for example, in ^{13}C (Ref. 2) or in ^{17}O and ^{18}O (Refs. 6–8).

2. *The major peak at 15.5 MeV*

The $(\gamma,1n)$ cross section peaks at 15.5 MeV at a value of 9.1 mb. The average neutron energy for this region is consistent with that expected if most transitions proceed to the ground state of ^{13}C. It is reasonable to suggest, therefore, that single 1p-1h excitations of the $p_{1/2}$ neutrons dominate the reaction here.

Above 15.5 MeV, the $(\gamma,1n)$ cross section decreases but maintains its dominant ground-state character until about 17.5 MeV, where the average (single) photoneutron energy drops significantly. In the region from 19 to 20 MeV, the average photoneutron energy is seen to lie between about 6 and 7 MeV. This suggests that very few transitions in this energy region proceed to the ground state of ^{13}C (which would result in the emission of 10- to 11-MeV neutrons) and that most go to excited states near 4 MeV in ^{13}C. The $\frac{3}{2}^-$ state is a likely candidate, so that $p_{3/2}$ neutron transitions from the core s-d shell would appear to be dominant.

3. *The region from 22 to 27 MeV*

The single photoneutron cross section begins to fall near 22.5 MeV to a deep minimum centered just below 27 MeV. This decrease can be accounted for by the opening of the (γ,p) channel at 20.8 MeV, and photoprotons with enough energy to overcome the Coulomb barrier are now available to participate in the deexcitation process.

The $(\gamma,2n)$ cross section, whose threshold is 13.12 MeV, has little strength below 23.3 MeV [see Fig. 3(c)]. Above this energy, decay to the $T=\frac{3}{2}$ state at 15.11 MeV in ^{13}C becomes energetically possible. The large $T_>$ component of ^{14}C that is predicted by most calculations (e.g., see Refs. 19–21) now can decay via isospin-allowed transitions to the 15.11-MeV state in ^{13}C. This state then decays by neutron emission.

Therefore, the significant dip in the $(\gamma,1n)$ cross section near 26.5 MeV can be attributed to the onset of both the (γ,p) and $(\gamma,2n)$ channels for the decay of the (presumed) $T_>$ part of the GDR.

4. *The region above 27 MeV*

Above 27 MeV, the single photoneutron cross section rises again because of the opening of the (γ,pn) channel at 25.7 MeV and because the Coulomb barrier for proton emission [in the sequential (γ,pn) reaction, for example] is less important in the competition with the isospin selection rules inhibiting the $(\gamma,2n)$ reaction (assuming, as discussed in the preceding section, that the GDR in this energy region is largely $T_>$), except for those $(\gamma,2n)$ events that proceed through the relatively few $T=\frac{3}{2}$ states (including the 15.11 MeV state) available in ^{13}C. As the energy increases, the (γ,pn) process becomes favored rapidly (the Coulomb barrier is overcome more quickly than the density of $T=\frac{3}{2}$ states in ^{13}C increases) and soon dominates the decay of the $T_>$ giant resonance. Thus, these data are consistent with the hypothesis that a large part of the absorption cross section in this energy region consists of $T_>$ strength.

Above 29 MeV, $(\gamma,2n)$ reactions can proceed directly to the first $T=1$ state in ^{12}C by direct two-neutron emission and can (but do not necessarily) begin to compete again with the (γ,pn) channel. However, this direct (rather than sequential) process is inhibited by phase-space considerations because direct two-neutron emission results in a three-body (rather than a two-body) final state.

B. The $(\gamma,2n)$ cross section

As can be seen in Fig. 3(c), the $(\gamma,2n)$ cross section rises slowly from its threshold at 13.1 MeV. There is little evidence of any strength at 15.5 MeV, the maximum of the

$(\gamma,1n)$ cross section. For energies below 23.3 MeV, transitions to $T=\frac{3}{2}$ states in ^{13}C are not possible (the first $T=\frac{3}{2}$ state in ^{13}C is at 15.11 MeV). Therefore, it is reasonable that the $(\gamma,2n)$ cross section below this energy exclusively represents photoabsorption to $T_<$ states in ^{14}C which decay via the sequential emission of two neutrons. From the average photoneutron energies shown in Fig. 4(b), it appears that ground-state transitions to ^{12}C dominate the cross section up to about 20 MeV.

At about 20 MeV there is a distinct increase in the $(\gamma,2n)$ cross section, accompanied by a leveling off of the average $(\gamma,2n)$ photoneutron energy. This suggests the onset of transitions to excited states in ^{12}C, possibly arising from population of states of a more complex nature in ^{14}C. This effect, predicted by the calculation of Ref. 19, was observed in the single-neutron channel and might be attributed to the dominance of transitions from the $p_{3/2}$ shell. It might also be accounted for by the onset of the $T_>$ part of the GDR combined with an increased mixing of $T_>$ and $T_<$ components of these states in ^{14}C. This would permit decay of $T_>$ strength to $T=\frac{1}{2}$ states in ^{13}C and thence to $T=0$ states in ^{12}C. As soon as the isospin selection rule allows transitions from $T_>$ states, the $(\gamma,2n)$ cross section rises rapidly to its peak at 26 MeV and dominates the other open channels [(γ,n) and (γ,pn)]. This observation is in excellent qualitative agreement with the theoretical prediction of Kissener *et al.*,[19] and signifies that most of the $(\gamma,2n)$ cross section above approximately 24 MeV represents excitation of $T_>$ states. As discussed above, the $(\gamma,2n)$ cross section dies away as the (γ,pn) channel effectively opens at $\sim$27 MeV.

C. The total photoneutron cross section

Figure 3(a) shows the sum of the $(\gamma,1n)$ and $(\gamma,2n)$ cross sections. It is tempting to associate the two obvious resonance structures, one [in $\sigma(\gamma,1n)$] near 15.5 ± 0.5 MeV and the other [in $\sigma(\gamma,2n)$ and perhaps $\sigma(\gamma,pn)$] near 25.5 ± 1.0 MeV with the $T_<$ and $T_>$ components of the GDR, respectively. On this assumption, the magnitude of the isospin splitting of the GDR would be about 10 MeV. According to Fallieros and Goulard,[22] the energy centroids of the two isospin components of the GDR should be separated by an energy $\Delta E\approx 60(T_0+1)/A$ MeV, which is 8.6 MeV for the case of ^{14}C ($T_0=1$). However, this isospin reconstruction cannot be carried out completely until the total photon absorption cross section is known, and this requires knowledge of the other major decay channel, the (γ,p) reaction.

D. Integrated cross sections and sum rules

Figure 6 presents the measured integrated cross sections and their energy-weighted moments for the $(\gamma,1n)$, $(\gamma,2n)$, and (γ,n_{tot}) reactions, computed from

$$\sigma_{int}=\int\sigma(E_\gamma)dE_\gamma\ ,$$

$$\sigma_{-1}=\int\sigma(E_\gamma)E_\gamma^{-1}dE_\gamma\ ,$$

and

$$\sigma_{-2}=\int\sigma(E_\gamma)E_\gamma^{-2}dE_\gamma\ .$$

The curves in this figure may be used to obtain values of the integrated cross section between any two photon energies up to 36 MeV, the maximum energy of this experiment.

Table II presents a comparison of the values of σ_{int} for ^{14}C with those for other *p*- and *s-d*-shell nuclei, integrated up to 30 MeV. The present results are consistent with the systematics observed in these neighboring nuclei. For both the carbon and oxygen isotopes the integrated total photoneutron cross section increases significantly as one, and then two, neutrons are added to the (^{12}C and ^{16}O) "cores."

The present measurement provides no new information regarding the integrated total photonuclear cross section in this mass region until it can be supplemented with a measurement of the $^{14}C(\gamma,p)$ cross section. Systematics suggest that the proton decay channel is likely to be responsible for approximately 25% of the total photon ab-

TABLE II. Photonuclear cross sections integrated up to 30 MeV. Compilation from Ref. 3 except where indicated.

Nucleus	$\int\sigma(\gamma,n_{tot})dE_\gamma$ (MeV mb)	TRK units	$\int\sigma(\gamma,p)dE_\gamma$ (MeV mb)	TRK units	Sum TRK units
^{12}C	42	0.23	72	0.40	0.63
^{13}C	95	0.49	42[a]	0.22	0.71
^{14}C	108[b]	0.53	not available		
^{14}N	99	0.47	15	0.07	0.54
^{15}N	90	0.40	70	0.31	0.71
^{16}O	55[c]	0.23	91	0.38	0.61
^{17}O	95	0.37	52[d]	0.2	0.6
^{18}O	142	0.53	31	0.12	0.65

[a]Reference 12 (extrapolated from 28 MeV).
[b]Present work.
[c]Reference 5.
[d]Preliminary result (Ref. 14).

sorption cross section in ^{14}C, but this needs to be verified experimentally.

E. Comparison with theoretical predictions

A comparison of the present measurement with recent shell-model calculations is presented in Fig. 7. The calculation of Kissener *et al.*,[19] which uses a phenomenological interaction (Cohen-Kurath matrix elements and Gillet's interaction CAL), predicts the strength and distribution of the $T_<$ and $T_>$ $J^\pi=1^-$ states. A width of 2 MeV has been assigned to a Lorentz convolution of each dipole state to produce the curves shown in Fig. 7(a).

The prediction of a recent particle-hole calculation by Assafiri and Morrison[21] is shown in Fig. 7(b). This calculation was carried out under the dipole approximation, using the residual nucleon-nucleon interaction of Cooper and Eisenberg[26] and a well depth of 50 MeV. A monotonically increasing width (from 750 keV at 13 MeV to 4 MeV at 30 MeV) has been assigned to a Lorentz convolution of each dipole state to produce the curve shown in Fig. 7(b). Both of these calculations give approximately the same shape for the photon absorption cross section except that the absolute cross-section scale of the calculation by Kissener *et al.* is larger by a factor of about 4.

In the results of both calculations, a few $T_<$ states cluster around 15 MeV to produce a peak which is comparable to that observed in this experiment. This is consistent with the fact that the strength seen in the experimental cross section around 15 MeV is almost certainly $T_<$. This is because the average photoneutron energy in this energy region is high, indicating predominantly ground-state or near-ground-state transitions [see Fig. 4(a)]; since decay of $T_>$ states to $T=\frac{1}{2}$ states in ^{13}C is isospin forbidden, the states in this energy region must have $T=T_<$.

Below the (γ,p) threshold (at 20.83 MeV), the agreement between the measured and calculated energies of the resonances is quite good. The magnitude of the calculated results of Assafiri and Morrison is in better agreement with the experimental data than the calculated results of Kissener *et al.*, but it still overestimates the magnitude of the cross section. Somewhat better agreement would have been achieved if a slightly larger width had been used for the Lorentz convolution in this energy region.

Both of the calculations predict that nearly all of the $T_>$ strength is concentrated in a few states near 26 MeV. The measured total photoneutron cross section is not markedly concentrated in this energy region [although the $(\gamma,2n)$ cross section is indeed sharply peaked at 26 MeV]. However, it might turn out that much of this predicted absorption strength will appear in the photoproton reaction channel.

F. Comparison with ^{12}C, ^{13}C, and the oxygen isotopes

Considering ^{12}C and ^{16}O as closed-shell nuclei, it is instructive to compare the photoneutron cross sections of the isotopes obtained by adding valence neutrons to these "cores." All of these photoneutron cross sections are shown in Fig. 8.

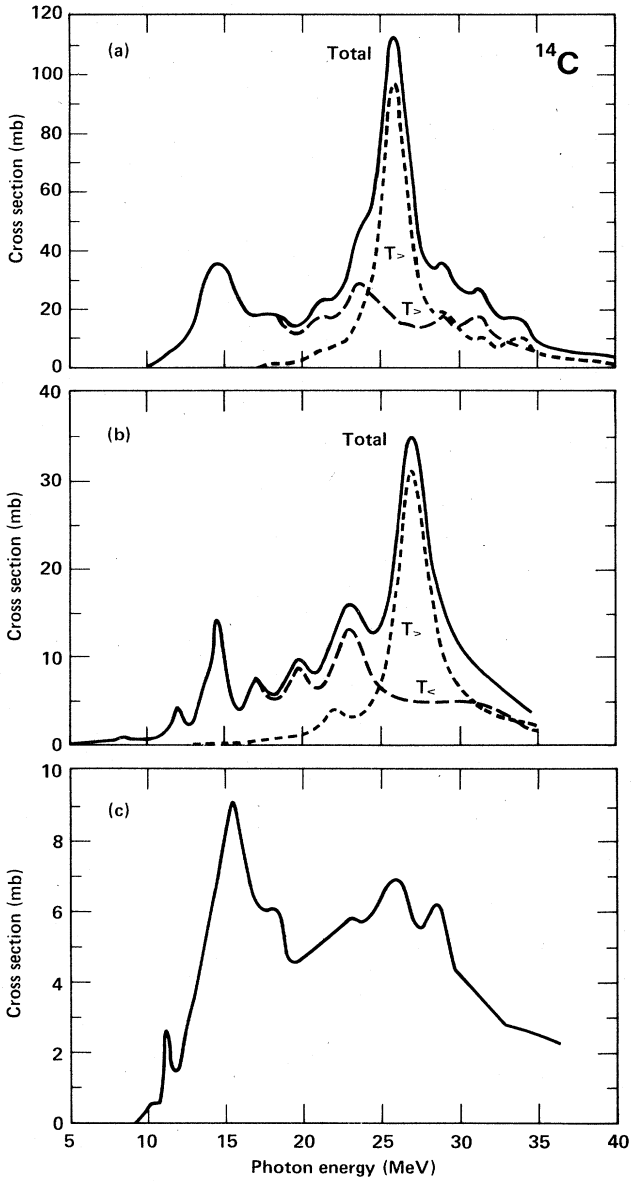

FIG. 7. The predictions of (a) the shell-model calculations of Kissener *et al.* (Refs. 19) and (b) those of Assafiri and Morrison (Ref. 21) are shown compared with (c) the present experimental results for the $^{14}C(\gamma,n_{tot})$ cross section.

With the addition of a neutron to ^{12}C, the $^{13}C(\gamma,n_{tot})$ cross section exhibits a "classic" pygmy resonance at energies below the GDR. This is a similar situation to that seen in ^{17}O where a valence neutron is added to the ^{16}O "core." In contrast, the $^{14}C(\gamma,n_{tot})$ cross section is strikingly different from the $^{18}O(\gamma,n_{tot})$ cross section even though both nuclei may be considered to contain two neutrons outside a closed "core." The $^{18}O(\gamma,n_{tot})$ cross section consists of a prominent GDR with some strength at energies below the GDR. On the other hand, the major strength in the ^{14}C cross section appears where (on the basis of the situation in ^{18}O) one might expect the pygmy

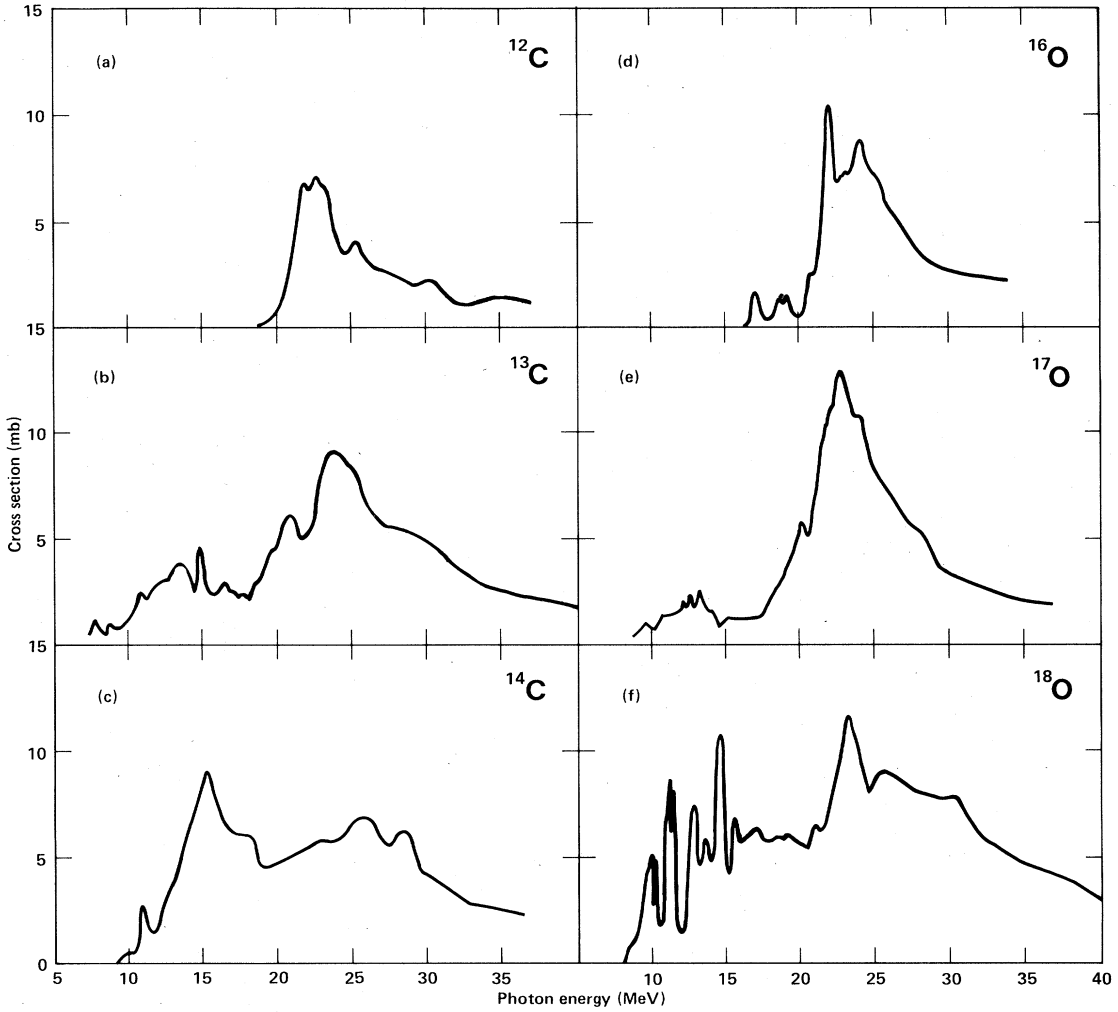

FIG. 8. A comparison of the total photoneutron cross sections for (a) ^{12}C (Ref. 1), (b) ^{13}C (Ref. 2), (c) ^{14}C (present result), (d) ^{16}O (Ref. 5), (e) ^{17}O (Ref. 6), and (f) ^{18}O (Refs. 7 and 8).

resonance to occur. From the theoretical predictions shown in Fig. 7, as well as the systematics observed in Fig. 8, one might expect the major strength in the ^{14}C(γ,n_{tot}) cross section to lie near 25 MeV. This is not the case. The second major difference between the ^{14}C and ^{18}O cross sections is that the strength at energies below the GDR in ^{18}O is fragmented into many narrow peaks. This feature is not seen in ^{14}C, where the cross section in the energy region between 10 and 20 MeV is relatively featureless. This effect also is observed in the ground-state cross section.[18]

However, the distribution of the photoneutron cross-section strength in ^{14}C is not an unambiguous signature of the closed-shell nature of the nucleon configuration in ^{14}C. It still is possibly just a natural consequence of the decay of the total absorption cross section consistent with kinematic, isospin, and Coulomb-barrier constraints, as has been discussed in the preceding sections. A measurement of the ^{14}C(γ,p) cross section is needed to clarify this situation definitively.

IV. SUMMARY

The photoneutron cross sections for ^{14}C have been measured with monochromatic photons from threshold to 36 MeV. The gross structure seen in these cross sections can be explained in terms of the reaction kinematics coupled with the competition between the various particle decay channels and the expected isospin splitting of the GDR. A sharp peak observed at 11.3 MeV appears to have a significant $M1$ component.

The present measurement is consistent with the calculations of Kissener *et al.* and of Assafiri and Morrison in terms of the gross location, but not the distribution, of both the absorption strength and the two isospin components of the GDR.

The total photoneutron cross section for ^{14}C does not show the typical pygmy resonance, as would be expected in the standard weak-coupling model. However, this is not necessarily indicative of the closed- or unclosed-shell nature of ^{14}C. A definitive interpretation with reference

to all of the above points, however, cannot be made until the photoproton cross section, and hence the total photonuclear cross section, of ^{14}C is known.

ACKNOWLEDGMENTS

We wish to thank Helmut Baer (LANL) for sample packaging, Paul Meyer (LLNL) for assistance with the experimental setup, and Youseff Assafiri and Ian Morrison for making available the result of their calculations in advance of publication. This work was performed at the Lawrence Livermore National Laboratory under the auspices of the U.S. Department of Energy under Contract No. W7405-ENG-48 and was supported in part by the Natural Sciences and Engineering Research Council of Canada, the University of Melbourne, and the University of Saskatchewan.

[1]S. C. Fultz, J. T. Caldwell, B. L. Berman, R. L. Bramblett, and R. R. Harvey, Phys. Rev. **143**, 790 (1966).
[2]J. W. Jury, B. L. Berman, D. D. Faul, P. Meyer, K. G. McNeill, and J. G. Woodworth, Phys. Rev. C **19**, 1684 (1979).
[3]J. W. Jury, B. L. Berman, J. G. Woodworth, M. N. Thompson, R. E. Pywell, and K. G. McNeill, Phys. Rev. C **26**, 777 (1982).
[4]J. T. Caldwell, R. L. Bramblett, B. L. Berman, R. R. Harvey, and S. C. Fultz, Phys. Rev. Lett. **15**, 967 (1965).
[5]B. L. Berman, J. W. Jury, J. G. Woodworth, R. E. Pywell, K. G. McNeill, and M. N. Thompson, Phys. Rev. C **27**, 1 (1983).
[6]J. W. Jury, B. L. Berman, D. D. Faul, P. Meyer, and J. G. Woodworth, Phys. Rev. C **21**, 503 (1980).
[7]J. G. Woodworth, K. G. McNeill, J. W. Jury, R. A. Alvarez, B. L. Berman, D. D. Faul, and P. Meyer, Phys. Rev. C **19**, 1667 (1979); LLNL Report UCRL-77471, 1978 (unpublished); B. L. Berman, D. D. Faul, R. A. Alvarez, and P. Meyer, Phys. Rev. Lett. **36**, 1441 (1976).
[8]R. E. Pywell, M. N. Thompson, and B. L. Berman, Nucl. Instrum. Methods **178**, 149 (1980).
[9]R. E. Pywell, B. L. Berman, J. W. Jury, J. G. Woodworth, K. G. McNeill, and M. N. Thompson, Phys. Rev. C **27**, 960 (1983).
[10]R. E. Pywell, B. L. Berman, P. Kean, and M. N. Thompson, Nucl. Phys. **A369**, 141 (1981).
[11]G. Odgers, B. L. Berman, R. E. Pywell, and M. N. Thompson, Nucl. Phys. **A288**, 445 (1982).
[12]D. Zubanov, R. A. Sutton, M. N. Thompson, and J. W. Jury, Phys. Rev. C **27**, 1957 (1983).
[13]J. E. E. Baglin and M. N. Thompson, Nucl. Phys. **A138**, 73 (1969); R. C. Morrison, J. R. Stewart, and J. S. O'Connell, Phys. Rev. Lett. **15**, 367 (1965).
[14]D. Zubanov, M. N. Thompson, B. L. Berman, J. W. Jury, R. E. Pywell, and K. G. McNeill, private communication.
[15]H. Crannell, J. M. Finn, P. Hallowell, J. T. O'Brien, N. Ensslin, L. W. Fagg, E. C. Jones, Jr., and W. L. Bendel, Nucl. Phys. **A278**, 253 (1977).
[16]M. C. Wright, H. Kitazawa, N. R. Robertson, H. R. Weller, M. J. Jensen, and D. R. Tilley, Bull. Am. Phys. Soc. **28**, 650 (1983).
[17]R. O. Lane, H. D. Knox, P. Hoffmann-Pinther, R. M. White, and G. F. Auchampaugh, Phys. Rev. C **23**, 1883 (1981).
[18]P. C-K. Kuo, K. G. McNeill, N. K. Sherman, S. Landsberger, W. F. Davidson, J. W. Jury, and J. R. C. Lafontaine, Phys. Rev. C **31**, 318 (1985); and private communication.
[19]H. R. Kissener, R. A. Eramzhyan, and H. U. Jager, Nucl. Phys. **A207**, 78 (1973); H. R. Kissener and R. A. Eramzhyan, *ibid.* **A326**, 289 (1979).
[20]J. D. Vergados, Nucl. Phys. **A239**, 271 (1975).
[21]Y. I. Assafiri and I. Morrison, Nucl. Phys. **A427**, 460 (1984).
[22]S. Fallieros and B. Goulard, Nucl. Phys. **A147**, 593 (1970); B. Goulard and S. Fallieros, Can. J. Phys. **45**, 322 (1961).
[23]A. H. Wapstra and K. Bos, At. Data Nucl. Data Tables **19**, 215 (1977).
[24]R. L. Bramblett, J. T. Caldwell, B. L. Berman, R. R. Harvey, and S. C. Fultz, Phys. Rev. **148**, 1198 (1966); R. E. Sund, V. V. Verbinski, H. Weber, and L. A. Kull, Phys. Rev. C **2**, 1129 (1970); H. Beil, R. Bergère, P. Carlos, A. Leprêtre, A. Veyssière, and A. Parlag, Nucl. Phys. **A172**, 437 (1971); L. M. Young, Ph.D. thesis, University of Illinois, 1972 (unpublished).
[25]S. Mordechai, H. T. Fortune, G. E. Moore, M. E. Cobern, R. V. Kollaritz, and R. Middleton, J. Phys. G **4**, 407 (1978); Nucl. Phys. **A301**, 463 (1978).
[26]B. S. Cooper and J. M. Eisenberg, Nucl. Phys. **A114**, 184 (1968).
[27]R. E. Pywell, B. L. Berman, J. G. Woodworth, J. W. Jury, K. G. McNeill, and M. N. Thompson, Phys. Can. **40**, No. 3, 68 (1984).